Supplementary Information for:

"Morphology evolution via self-organisation and lateral and vertical diffusion in polymer:fullerene solar cell blends"

Mariano Campoy-Quiles*, Toby Ferenczi*, Tiziano Agostinelli†, Pablo G. Etchegoin††, Youngkyoo Kim*, Thomas Anthopoulous*, Paul N. Stavrinou*, Donal. D. C. Bradley* and Jenny Nelson*

Here we explain the analysis of the ellipsometry data obtained for P3HT:PCBM blend films and provide justification for the morphology model presented.

In order to obtain the complex refractive indices and thicknesses of a multilayer structure from ellipsometry data a mathematical model is needed [23]. For the case of a thin film deposited on a substrate of known optical constants (such as quartz [36]), an initial guess for the refractive index and thickness of the thin film is used as the starting point in an iterative process that minimises the difference between the modelled and experimental ellipsometric data. The standard deviation (σ) of the fitting process serves as a parameter that quantifies the quality of the fit: the smaller the σ value, the better fit.

Our approach is summarised as follows: first, we characterise separately the optical constants of the two components using established descriptions of the dielectric function of conjugated polymers. Then, we consider a number of different models for the blend film, evaluating these models in terms of the standard deviation of the fitted ellipsometry data, relative to the number of fitting parameters used. Here, the models are applied to data for a series of six films spin coated for different lengths of time, producing morphologies representative of the range between "untreated" (long spinning time) and slow dried (short spinning time). The model which leads to the lowest standard deviation (σ) and consistently performs the best consists of a vertically graded blend of P3HT and PCBM underneath a homogeneous blend layer of PCBM and air.

Characterisation of individual components

We have fabricated spin coated films of the pristine materials on quartz and recorded their ellipsometric data for three incidence angles over an extended visible spectrum (from 250 to 850 nm). The data were analysed using the Standard Critical Point (SCP) model, which has been successfully used previously to characterise the optical constants of 5 polyfluorene copolymers [36]. The refractive index of PCBM was described using 3 exciton lineshapes. For pristine P3HT, 5 peaks were included, 2 excitons (UV-blue region) and 3 one-dimensional critical points (visible region). The inclusion of the 1D peaks improves the fit of the ellipsometry data with respect of the use of excitons. This is consistent with the reported results that suggest that spin coated pristine P3HT films are polycrystalline rather than amorphous, i.e. they have a macromolecular ordering. The imaginary part of the refractive index, also known as the extinction coefficient, of P3HT (PCBM) is shown in red (blue) in Fig. SI 1a.

Modelling of blend films

The models tried are listed in Table S1. Each model consists of a blend layer of P3HT:PCBM, in some cases underneath a blend of PCBM and air. The latter is introduced to represent scattering by PCBM aggregates which are observed to protrude from the film surface (Fig. 2.4 and Ref. [17]). Fig. S1 c-f present schematics of four of the models considered. Each model is characterised by a number of fitting parameters which are to be optimised. We have used the Bruggeman effective medium approximation to characterise the blends reported here. Other models such as Maxwell Garnett, Lorentz-Lorenz and Ping Sheng have also been studied for completeness, and they led to consistent results within the error bars deduced for the parameters.

The models were applied to the measured ellipsometric data for a series of 6 films that were fabricated from the same P3HT:PCBM (1:1) solution in CB, where the spin speed was kept constant (2000 r.p.m.) while the spinning time was varied from 80 seconds to 3 seconds. This is equivalent to moving from an untreated film (>30 s) to a slow dried film (<15 s). The corresponding standard deviations for the fits are shown in Fig. SI 1b.

Discussion

Describing the blend film as a homogeneous distribution of the two components yields relatively high σ's (black solid triangles in Fig. SI 1b), particularly for slow dried films.

Assuming a gradient of concentration through the film, such that the PCBM concentration decreases from substrate to free surface, generally improves σ (green solid squares in Fig. SI 1b for linear profiles). Graded films are mathematically realised by dividing the blend film into a finite number of sublayers with varying relative concentration and thickness depending on the specific profile. It can be shown that for this type of blend, and in the range of thickness considered (around 30-80 nm), the improvement in σ converges for around 5 sublayers. A better fit than for the homogeneous case is, however, expected since we are increasing the number of fitting parameters. We note that if we force the model to have the opposite gradient, σ increases more than 3 fold with respect to the homogeneous blend, supporting the reliability of the fitting procedure. Other graded profiles requiring more fitting parameters were used but did not result in any significant improvement in the quality of the fit compared to the linear case.

The inclusion of a PCBM:void layer on the top of a homogeneous blend layer yields better σ (open blue squares) than both the homogeneous and graded models. This layer introduces scattering in the polarisation of light during the ellipsometry experiments. Alternatively, a rough interface would also scatter the incident beam mixing the two polarisations. However, a rough interface, which is realised by a blend of void and (P3HT:PCBM (1:1)), did not improve the fit at all with respect to the homogeneous blend, further suggesting that the protruding aggregates consist of PCBM only.

As the spinning (drying) time becomes shorter (larger), the three models described above start failing. It is only when we combine a graded profile in the blend topped with a PCBM:void scattering layer (red open triangles) that the fit is good for all conditions, which is reflected as a nearly constant (and the lowest) σ value at all spinning times. This is therefore the most general description of our system. In fact, the same model gave consistently lower σ values than the other three models for all the samples investigated in this paper, including thermally annealed films, vapour annealed samples, films deposited using different spin speeds (from 700 r.p.m. to 5000 r.p.m.), and films deposited on different substrates (quartz, PEDOT covered quartz and SAM coated Si/SiO_2 substrates). We note that this model requires five fitting parameters: thickness, linear slope and average concentration of the blend layer, and thickness and PCBM average concentration for the top layer. We found that other models characterised by five parameters, such as a single graded blend layer with an exponential profile, did not lead to this level of improvement in the quality of the fit, giving further confidence to our choice of mathematical description of P3HT:PCBM blends.

The range of composition profiles deduced from this model is represented in Fig. 3a-d. To give one last example, Fig. SI 2 shows the graded profile of PCBM for a spin coated P3HT:PCBM blend film on quartz before (blue line) and after (red line) vapour annealing. Consistent with the cases of thermal annealing and slow drying (see main text), the slope becomes more pronounced upon annealing, and the amount of PCBM present in the upper PCBM:void layer increases.

Rigorous coupling wave analysis

We have further checked the sensitivity of ellipsometry and photometry to detect vertical and lateral phase separation by using rigorous coupling wave. The two case studies were a periodic lateral phase separation of varying period, and a vertically separated blend film. The main conclusion of this investigation is that vertical and lateral segregations can be detected using both photometry and ellipsometry. The larger deviations with respect to a homogeneously distributed blend occur for wavelengths within the absorption spectral region of the materials. We note that the sensitivity of these techniques to lateral phase separation is limited to average domain sizes larger than the wavelength of light. The details of these calculations will be presented elsewhere.

Analysis of Al covered blend films

In order to investigate the effects of Al evaporation on the morphology of P3HT:PCBM blend films, we evaporated an ultrathin (circa 8 nm) optically semitransparent Al layer on top of as spin coated and annealed (140^{o}C for 40 minutess) blend films. Half of each sample was covered with Al while the remaining half was kept Al free in order to have the most accurate reference possible (Fig. SP 3a). Optical micrographs (Fig SP 3b,c) show that PCBM clusters can be found on both sides –Al free and Al coated-, although the size of cluster seems larger for the Al free side. Thicker Al films would be required in order to homogenously cover the blend films, but these would need to have thicknesses in excess of 25 nm (according to theoretical calculations and the average size of PCBM clusters), which would then make these Al layers optically opaque and thus unsuitable for non destructive optical examinations. Figure SP 3d shows the best model for the analysis of ellipsometry data for a 40 nm thick spin coated P3HT:PCBM blend film on quartz with a 8 nm thick Al layer evaporated on top. This blend was annealed before the evaporation of the contact. The resulting model clearly shows how the PCBM clusters go beyond the thin Al layer. As can be seen in Figure SI 3e, the slope of the film remains unchanged when the Al layer is evaporated on top of the film. The analogous case of a spin coated (non-annealed) blend covered with Al is shown in Fig. SI 3f, and similar conclusions can be drawn. Annealing this last sample leads to diffusion of the PCBM as described in the main text for the Al free side of the film, but also substantial diffusion within the Al capped side. It is expected that thicker Al films would more severely restrict molecular mobility. Other protocols, such as thick Al layer removal using NaOH, or capping instead with thick layers of transparent materials, are being currently investigated in order to further explore the role of the contacts on the morphology of polymer:fullerene solar cells.

The comparative role of P3HT crystallisation and PCBM diffusion on solar cells

Figure SP 4 presents additional device characterisation data for samples annealed for different time intervals (0, 5 and 30 min). These serve as supporting information for the results presented in Table 1 and the discussion found in the main text.

Figure Captions

Figure SI 1a. Ellipsometrically deduced extinction coefficient of P3HT (red line) and PCBM (blue line); (b) Standard deviation of the fitting of the ellipsometric angles for six samples of P3HT:PCBM (1:1) spin coated onto quartz substrates at 2000 r.p.m. for different spinning times. The models used are a homogeneous blend (solid black triangles, schematically represented in Fig. SI 1c), a linear gradient of concentration blend (solid green squares, Fig. SI 1d), a homogeneous PCBM:void scattering layer on top of a homogeneous P3HT:PCBM blend (open blue squares, Fig. SI 1e), and a homogeneous PCBM:void scattering layer on top of a linear gradient of concentration blend (open red triangles, Fig. SI 1f).

Figure SI 2. Concentration profile of PCBM for a P3HT:PCBM blend deduced using a homogeneous PCBM:void scattering layer on top of a linear concentration profile for the blend film. The two lines represent the same film as spin coated (blue) and after vapour annealing for ~ 1 hour (red).

Figure SI 3. (a) Schematic top view of a sample half-covered with Al; Micrographs (around 200 microns in side) of a P3HT:PCMB annealed (140^{o}C for 40 min) film on the Al covered (b) and Al free (c) sides; (d) PCBM profile for an annealed blend deposited on top of a clean quartz substrate and topped with an evaporated 8 nm thick Al layer; (e) comparison between the PCBM profiles for an annealed P3HT:PCBM film sample on the Al coated (open triangles) and Al free (solid triangles) sides. Note that the analysis of the ellipsometric data was done using different models (see above); and (f) (e) comparison between the PCBM profiles for a spin coated P3HT:PCBM film sample on the Al coated (open triangles) and Al free (solid triangles) sides.

Figure SI 4. Optical density (a), current density vs. voltage curves (b) and EQE (c) for as spin coated (black solid line), annealed during 5 min (blue dashed line) and during 30 min (red dotted line) films and/or devices.

Table S1. Different models used to fit the ellipsometry data for a representative P3HT:PCBM blend film (spin coated on quartz at 2000 r.p.m. for 5 seconds).

Table S1.

Blend Layer	Type of Profile	Top Layer	# of Fitting parameters	Standard deviation [10^{-3}]
Homogeneous	None	None	2	3.98
Graded	Linear	None	3	2.51
Graded	Parabolic	None	4	2.19
Graded	Exponential	None	5	2.11
Homogeneous	None	PCBM:void	4	2.60
Graded	**Linear**	**PCBM:void**	**5**	**1.77**
Homogeneous	None	Blend:void	4	2.68
Graded	Linear	Blend:void	5	1.84

Figure SI 1

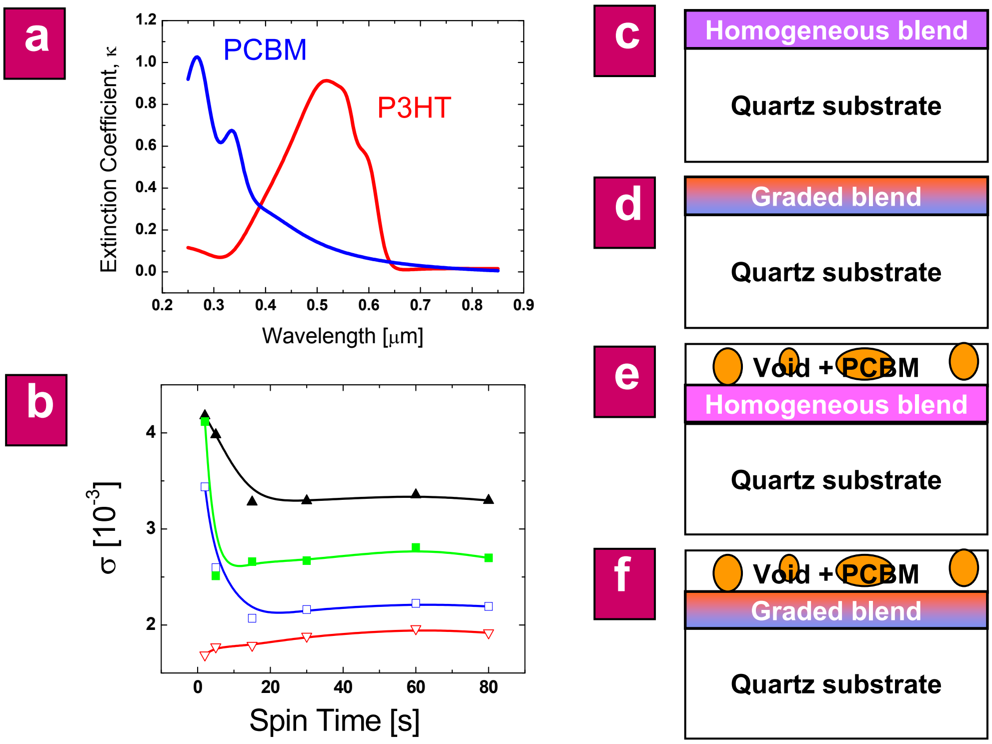
a
PCBM
P3HT
Extinction Coefficient, κ
Wavelength [μm]
b
σ [10^-3]
Spin Time [s]
c
Homogeneous blend
Quartz substrate
d
Graded blend
Quartz substrate
e
Void + PCBM
Homogeneous blend
Quartz substrate
f
Void + PCBM
Graded blend
Quartz substrate

Figure SI 2

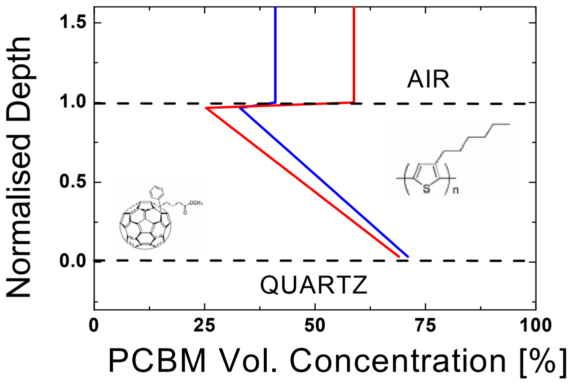

AIR
QUARTZ
Normalised Depth
PCBM Vol. Concentration [%]
0.0
0.5
1.0
1.5
0
25
50
75
100

Figure SI3

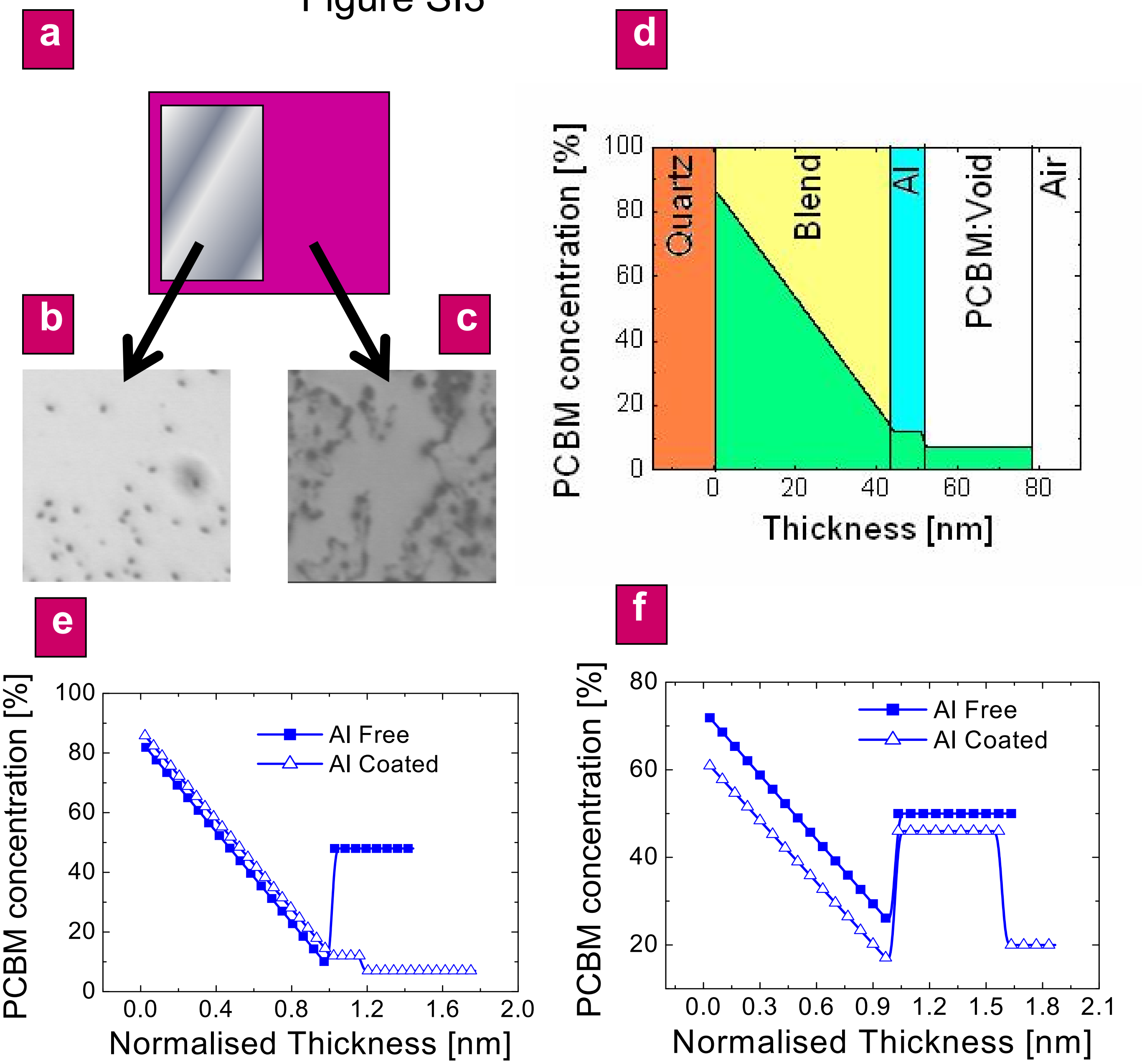
a
b
c
d
PCBM concentration [%]
Thickness [nm]
Quartz
Blend
Al
PCBM:Void
Air
100
80
60
40
20
0
0
20
40
60
80
e
PCBM concentration [%]
Normalised Thickness [nm]
Al Free
Al Coated
100
80
60
40
20
0
0.0
0.4
0.8
1.2
1.6
2.0
f
PCBM concentration [%]
Normalised Thickness [nm]
Al Free
Al Coated
80
60
40
20
0.0
0.3
0.6
0.9
1.2
1.5
1.8
2.1

Figure SI4

Table 1

Annealing time (min)	O.D. (520nm) (a.u)	Slope (on PEDOT) (%)	PCE (%)
0	0.709	-25.0	1.13
5	0.879	-6.8	3.64
30	0.879	-5.9	3.92

a

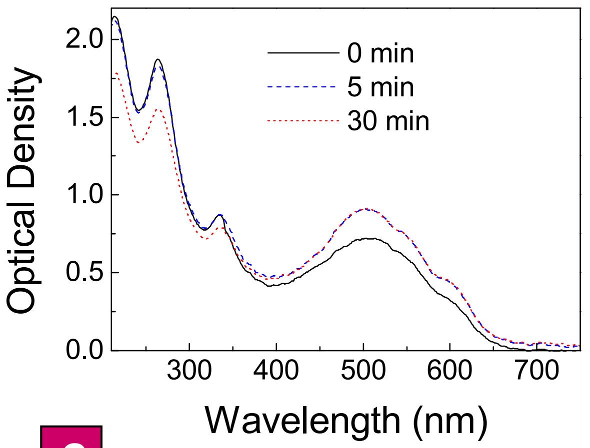

b

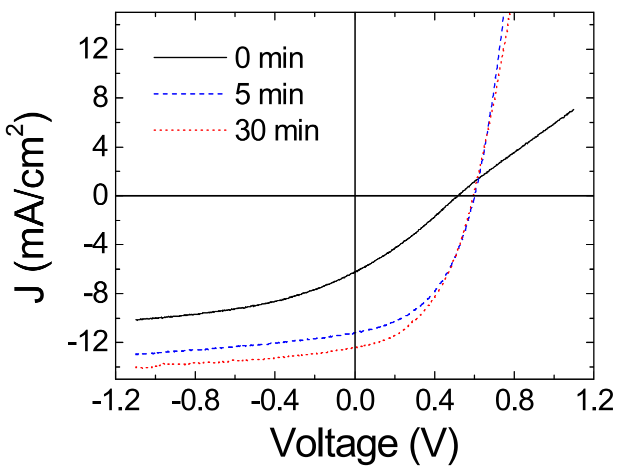

c